Shape Optimization of Dental Implants

Li Shi, BEng, MSc[1]/Haiyan Li, BEng, MSc, PhD[2]/Alex S. L. Fok, BEng, MSc, PhD, CEng[3]/Cemal Ucer, BDS, MSc[4]/ Hugh Devlin, BDS, BSc, MSc, PhD[5]/Keith Horner, BChD, MSc, PhD, FDSRCPS, DDR, FRCR[6]

Purpose: The purpose of this study was to derive alternative implant shapes which could minimize the stress concentration at the shoulder level of the implant. *Materials and Methods:* A topological shape optimization technique (soft kill option), which mimics biological growth, was used in conjunction with the finite element (FE) method to optimize the shape of a dental implant under loads. Shape optimization of the implant was carried out using a 2-dimensional (2D) FE model of the mandible. Three-dimensional (3D) FE analyses were then performed to verify the reduction of peak stresses in the optimized design. *Results:* Some of the designs formulated using optimization resembled the shape of a natural tooth. Guided by the results of the optimization, alternative implant designs with a taper and a larger crestal radius at the shoulder were derived. Subsequent FE analyses indicated that the peak stresses of these optimized implants under both axial and oblique loads were significantly lower than those observed around a model of commercially available dental implant. *Conclusion:* The new implant shapes obtained using FE-based shape optimization techniques can potentially increase the success of dental implants due to the reduced stress concentration at the bone-implant interface. INT J ORAL MAXILLOFAC IMPLANTS 2007;22:911–920

Key words: crestal bone loss, dental implant, finite element analysis, shape optimization

Placement of dental implants is a highly successful treatment for tooth loss, with a reported success rate of more than 99% for Straumann dental implants after 5 years in service[1] and 95% for Straumann solid-screw titanium implants placed in a clinical center and observed for up to 10 years.[2] However, these and other long-term studies[3] show that dental implants occasionally fail to remain osseointegrated, resulting in the loss of alveolar crestal bone. Crestal bone loss depends on many factors (eg, the biocompatibility of the implant, its geometry and surface characteristics, the surgical technique, the restorative treatment, and the loading conditions in relation to the quality and quantity of the surrounding bone).[4–9] Since bone has the ability to adapt its shape, through resorption and deposition, to the mechanical stimulus to which it is exposed, loading conditions have been considered one of the most important factors in implant success.[8,10] Experiments on animals have indeed shown resorption of the bone around oral implants to which excessive load was applied.[11–14]

The finite element (FE) method has been widely used to analyze the stress distribution of dental implants and the bone surrounding them.[15] Previous works have shown that a high level of stress can exist in the region of the bone around the neck of the implant.[16–20] Several factors could affect the stress level in the bone surrounding an implant. These include the applied loads, the quality and quantity of the bone, and the material and shape of the implant.[17–21] Since the bone quality and the applied loads are given factors which cannot be altered easily, choosing a dental implant of a favorable shape and/or material has been the focus of much research on reduction of the stress concentrations in the bone.[17,18,20,21] Many attempts have been made to optimize the shape of dental implants. Most have focused on increasing the diameter and/or the length of the implant to increase the contact area between the bone and implant, thereby reducing the stress level in the bone.[17,20,21] Optimal implant material has

[1]Doctoral Student, School of Mechanical, Aerospace and Civil Engineering, The University of Manchester, United Kingdom.
[2]Postdoctoral Researcher, School of Mechanical, Aerospace and Civil Engineering, The University of Manchester, United Kingdom.
[3]Senior Lecturer, School of Mechanical, Aerospace and Civil Engineering, The University of Manchester, United Kingdom.
[4]Doctoral Student, School of Dentistry, The University of Manchester, United Kingdom.
[5]Reader in Restorative Dentistry, School of Dentistry, The University of Manchester, United Kingdom.
[6]Professor of Oral and Maxillofacial Imaging, School of Dentistry, The University of Manchester, United Kingdom.

Correspondence to: Dr Alex S. L. Fok, School of Mechanical, Aerospace and Civil Engineering, The University of Manchester, PO Box 88, Sackville Street, Manchester M60 1QD, United Kingdom. Fax: +44 0161 274 4328. E-mail: alex.fok@manchester.ac.uk

Fig 1   2D FE mesh for a currently available implant.
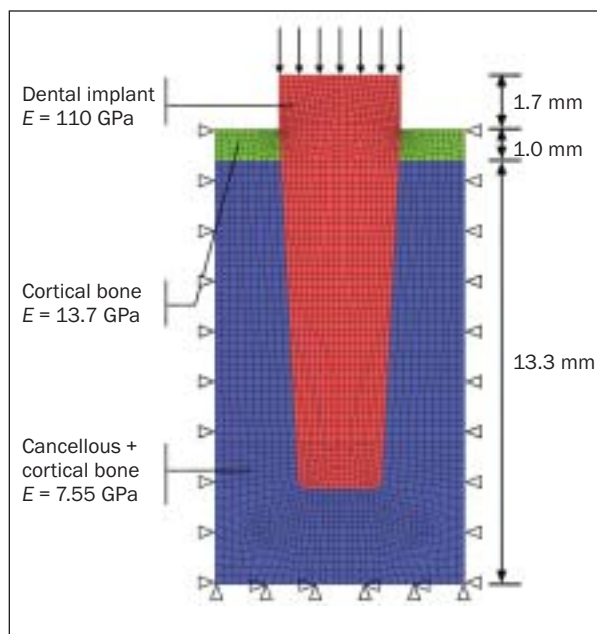
Table 1   Material Properties Used in the FE Model

	Young's modulus (GPa)	Poisson's ratio
Cortical bone[26]	13.7	0.3
Cancellous bone[26]	1.37	0.3
Implant (titanium)[15]	110	0.33

also been studied. For example, implants with functionally graded materials based on a combination of hydroxyapatite and titanium have been shown to reduce the stress concentration in the cortical bone and implants.[22] However, most of these implant designs were proposed on the basis of experience or intuition. Modern shape optimization technology has seldom been used as a tool for the design of dental implants, especially in the initial stage of draft design.

The first attempt to use optimization techniques for the design of dental restorations was probably that of Proos et al,[23] who considered the design of partial prostheses. More recently, Couegnat et al[24] studied the shape optimization of cavity preparations. The purpose of the present study was to employ topology optimization technology to derive alternative shapes for dental implants, with the aim of optimizing the stress distribution along the bone-implant interface. It is hoped that the new designs, which should result in lower stress concentrations, will help promote and maintain the osseointegration of dental implants.

MATERIALS AND METHODS

Preliminary FE Calculations

Figure 1 shows a 2-dimensional (2D) FE model (mesiodistal plane) of a currently available implant (Frialit-2; Friadent, Mannheim, Germany) which is placed into bone with a certain quality. This FE model was used to evaluate the stress levels in the bone induced by the loaded implant, especially in the area

around its neck. For simplicity, the screw thread was not modeled, and the bone and implant were considered to be bonded together perfectly along their interface. Also for simplicity, the bottom layer of cortical bone was not modeled, since the focus of this study was on the stress distribution around the neck of the implant. Preliminary calculations showed that the main results were not affected by the latter simplification. The imposed boundary conditions are also shown in Fig 1. The bottom face of the bone was restrained in both the vertical and horizontal directions, while the 2 vertical faces were restrained horizontally only. A pressure load giving a total axial force of 200 N was applied on the top surface of the implant, which represents the average maximum occlusal force for a partial prosthesis supported by implants in the molar region.[25] As the analysis was 2D, an out-of-plane thickness of 10 mm was assumed for the bone block, and a width of 4 mm was assumed for the implant.

The material properties of the bones[26] and implant[15] are shown in Table 1. Since a 2D model of the mesiodistal plane was employed, the stiffness of the bone structure underneath the top cortical layer would include contributions from the internal cancellous bone as well as the cortical bone on the buccal and lingual surfaces. The following formula was therefore used to calculate Young's modulus (E):

$$(1) \quad E = \frac{t_{can}E_{can} + t_{cor}E_{cor}}{t_{can} + t_{cor}}$$

where *t* is the out-of-plane thickness of the bone, and the subscripts "cor" and "can" represent "cortical" and "cancellous" bone, respectively. Based on a computerized tomographic (CT) scan image of a patient's jawbone, t_{can} was assumed to equal t_{cor}. Because Young's modulus of the implant was much higher than that of the other materials, similar contribution to the stiffness from the bone surrounding the implant was ignored. Using the aforementioned equation, Young's modulus for the cancellous bone region in the FE model (Fig 1) was calculated to be 7.55 GPa.

The commercial FE software ABAQUS[27] was used to perform the stress analysis. Eight-node plane-strain elements were used.

The Soft Kill Option in Structural Optimization

The implant shown in Fig 1 was optimized using a topology optimization method to reduce the stress concentration around its neck. Structural topology and shape optimization has been a very active research field,[28] and FE methods are the main tool used in topology optimization to generate optimal designs. With a design space, load sets, displacement sets, and a mass constraint, the most structurally efficient material layout can be determined using this kind of optimization. One of the simplest methods used in topology optimization is the so-called "soft kill option" (SKO), which was proposed by Mattheck[29] and has already gained wide acceptance in German industry. SKO mimics the biological mineralization process in living bone via FE modeling. Non–load-bearing material is carefully factored out in SKO according to the load distribution, thus providing a preoptimized lightweight design. This can be achieved computationally by following the flowchart shown in Fig 2.

Initially, the design space is filled with material of uniform Young's modulus, and the corresponding FE model under the anticipated loading condition is analyzed to obtain the stress distribution in the structure. Then, in the next FE analysis step, the local *E* value is set equal to a function of the stresses (σ) calculated at the particular point in the previous step, $E = f(\sigma)$, in which the function $f(\sigma)$ can be defined by the user. In most cases, *E* is set to be in proportion to the von Mises stress. In this way, the heavily loaded zones are strengthened and the lightly loaded zones are weakened, which is analogous to the deposition and resorption processes in living bone. After that, the new inhomogeneous structure is subjected to the same loading condition. The process is repeated until a converged state is achieved (ie, until the material is iteratively redistributed within the design space). The resulting material layout provides an optimal starting point for the design.
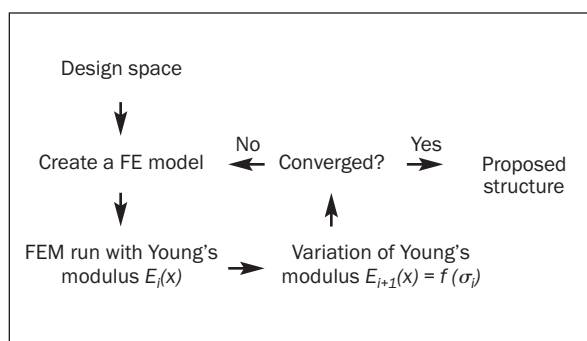

Fig 2 Flowchart of the SKO method.

The key in this process is the function $E = f(\sigma)$, which would affect both the results and the efficiency of the optimization process. Several functions have been proposed by Mattheck.[29] The simplest is the one-to-one function $E_{i+1} = \sigma_i$, where E_{i+1} and σ_i are the Young's modulus and stress determined in the (*i+1*)th *and i*th iteration, respectively. However, this function has low efficiency. Moreover, structures derived using this method have a wide range of Young's modulus values, which makes them difficult to manufacture.

An alternative method, the stress-increment-controlled method, was regarded as the best by Mattheck.[29] In this method, Young's modulus of an element was changed according to the following formula:

(2) $\quad E_{i+1} = E_i + k(\sigma_i - \sigma_{ref})$

where σ_{ref} is a reference stress. In the present case, this reference stress was used to divide the structure into areas of bone and areas of implant. The parameter *k* controls the rate of change of Young's modulus. The stress-increment-controlled method is highly efficient. In addition, the volume of the optimal structure can be controlled by changing the σ_{ref} value. However, the optimal structure still has a wide range of Young's modulus values. To avoid this problem in optimizing the shape of the dental implant, equations 3 and 4 were added to constrain the change of Young's modulus:

(3) $\quad E_{i+1} = E_1$ if $E_{i+1} < E_1$

(4) $\quad E_{i+1} = E_2$ if $E_{i+1} < E_2$

where E_1 and E_2 were the minimum and maximum values of Young's modulus, respectively, allowed in the structure. These additional equations ensure that there can only be 2 materials in the structure
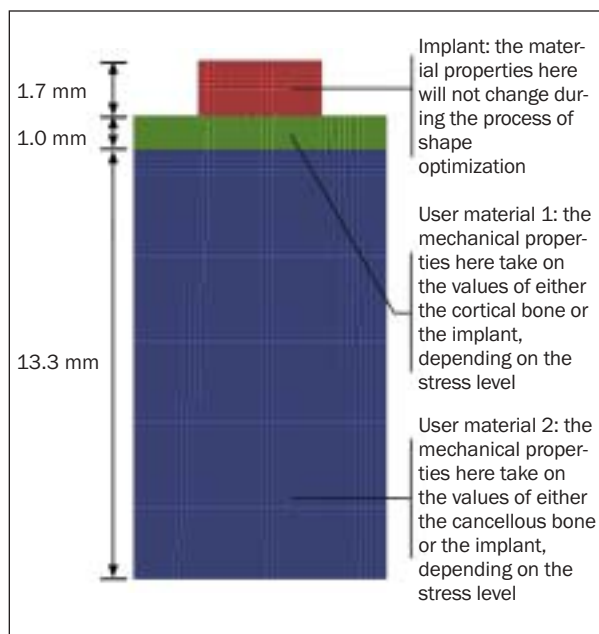
Fig 3 2D FE mesh and material distribution for optimizing the shape of a dental implant using the SKO process.

Fig 4 3D FE mesh for a currently available implant.

throughout the optimization process. In the present work, E_1 was Young's modulus of bone, either cortical or cancellous, depending on the region of the structure concerned, while E_2 was Young's modulus of the implant. The reference stress σ_{ref} was set as the maximum allowable stress in the bone, such that regions with stresses higher than this value would acquire properties of the implant. By selecting different E_1 or E_2 values, different qualities of bone and different materials for the implant could be considered.

The SKO process was implemented within ABAQUS[27] using a user material subroutine (UMAT) that can be used to define the constitutive behavior of a material for any procedure that includes mechanical behavior. It allows material properties to be modified by the applied loads during a stress analysis according to the principles defined by the user to suit their purposes. The function shown in equations 2 to 4 was thus programmed into a UMAT to automate the shape optimization process.

Figure 3 shows the 2D FE model and the initial material distribution used to derive optimal implant designs using the SKO method. The design space was formed by the external boundary of the model used in the preliminary stress analysis (Fig 1). A very fine mesh was employed to ensure accuracy of the solutions. Four-node plane-strain elements with a thickness of 10 mm were used in this part of the analysis. The boundary conditions were the same as those shown in Fig 1. Two user materials were defined: 1 for the cancellous bone region (E_{1can} = 7.55 GPa) and 1
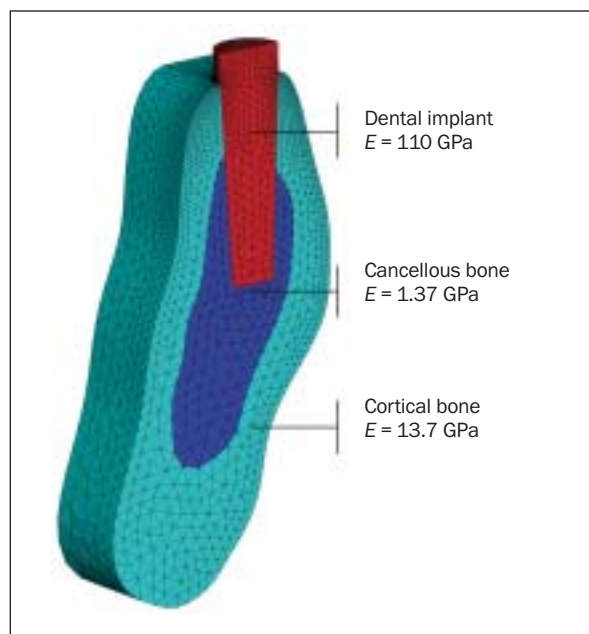
for the cortical bone region (E_{1cor} = 13.7 GPa). Analyses were performed using several values for the reference stress σ_{ref} (3, 4, 5, and 6 MPa) (ie, the maximum allowable stress in the structure). A lower reference stress is expected to produce optimized structures, with lower stresses along the implant-bone interface.

Further FE Analysis to Evaluate the Optimized Implant Design

Alternative implant designs were derived from the optimization process. Their effectiveness in reducing the stresses along the bone-implant interface was evaluated using further FE analysis, which included both 2D and 3D models. The latter allowed more realistic loading, with an oblique component in the buccolingual plane.

Because an actual implant has a cylindric shape, 2D FE analysis may not be adequate for accurate assessment of the stress levels in the bone. More FE analyses using 3D models (Fig 4) were therefore performed to confirm the reduction of the peak stresses in the optimized designs. The cross section of a mandible in the first premolar region was obtained from the CT images of a patient's jawbone. It was about 30 mm in height and 11 mm in width buccolingually. Using MSC-PATRAN,[30] the cross section was extruded to create the bone structure for a 3D model into which the implant was inserted. Since the geometry was symmetric about the buccolingual plane, only half of the implant and bone structure was modeled (Fig 4). Symmetric boundary conditions
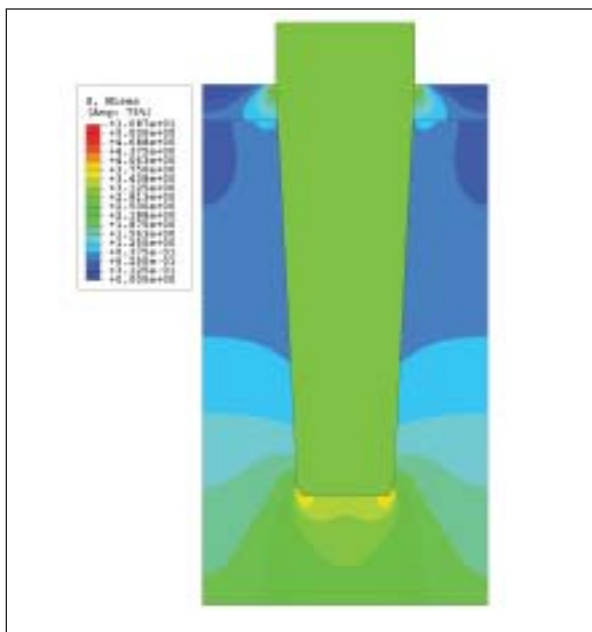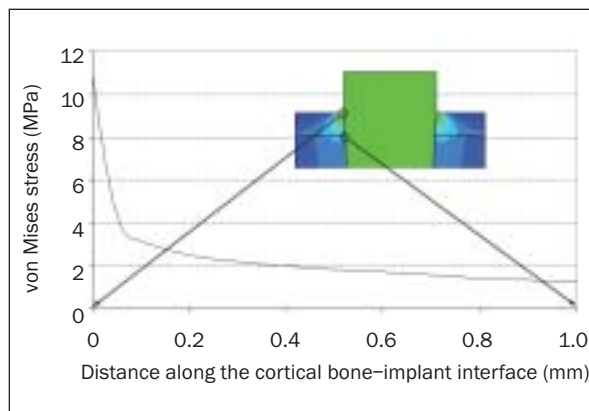
Fig 5 *(left)* Contours of von Mises stress induced by the original implant under axial loading.

Fig 6 *(below)* Von Mises stress along the cortical bone–implant interface under axial loading.

were thus used on the plane of mirror symmetry, while all three translational degrees of freedom were constrained on the other vertical cross-sectional plane of the model. The mesh around the neck of the implant was made finer than those in the other regions to accurately capture the stress concentration there, with an element edge length of about 0.1 mm. The 3D model contained 47,543 modified quadratic tetrahedral solid (C3D10M) elements and 118,316 nodes.

Oblique loading is considered most realistic and has been used by most researchers.[16,17] An oblique load with a 200-N vertical component and a 100-N horizontal component in the buccolingual direction was applied to the central node on the occlusal surface of the implant in the 3D models.[31]

RESULTS

Preliminary FE Calculations
Contours of the von Mises stress induced by an axial load of 200 N on the implant are shown in Fig 5 for the bone only; the stress contours in the implant are not shown for clarity. The values for the same stress entity along the cortical bone–implant interface are shown in Fig 6. The results show that high levels of stress, with magnitudes up to ~ 11 MPa, exist in the bone around the neck of the implant.

Theoretically, the stresses at a sharp corner or a point with material mismatch can be singular or infi-

nite. The FE predicted that values for the stresses at these points would depend on the mesh density there. Increasing the mesh density would lead to higher and higher predicted stresses at these points without ever achieving convergence. In order to make meaningful comparisons between different designs, therefore, the stresses along a length of the bone-implant interface in the vicinity of the stress concentration point were considered. This allowed comparison of the degrees of stress singularity, which is similar to the analysis of crack problems using fracture mechanics principles.

Shape Optimization Using SKO
The results from the optimization analysis were very sensitive to the reference stress. Different values of the reference stress produced structures with very different shapes. Figs 7a to 7d show the converged results in the form of distribution maps of Young's modulus for reference stresses of 3, 4, 5, and 6 MPa, respectively. It is interesting to see that the shapes obtained with a load of more than 4 MPa are similar to a natural tooth with 2 roots (Figs 7c and 7d). As the reference stress was decreased, the structure tended to rely further support from the fixed lower boundary (ie, to include an extended root). When the reference stress was 4 MPa, the 2 roots joined together to form a single column (Figs 7a and 7b). Reducing the reference stress further would increase the width of the column. Despite the very different shapes at the apical end, all the designs were quite similar in the
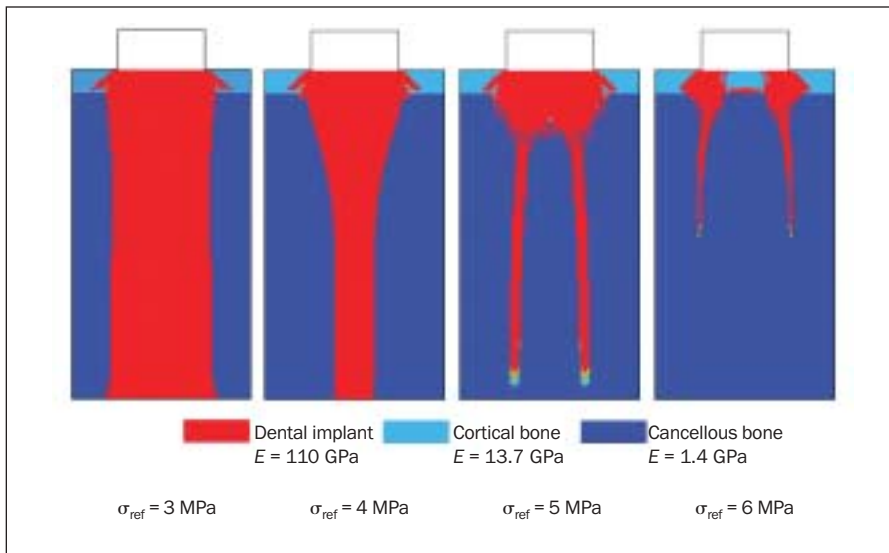
Dental implant
$E = 110$ GPa

Cortical bone
$E = 13.7$ GPa

Cancellous bone
$E = 1.4$ GPa

$\sigma_{ref} = 3$ MPa $\sigma_{ref} = 4$ MPa $\sigma_{ref} = 5$ MPa $\sigma_{ref} = 6$ MPa
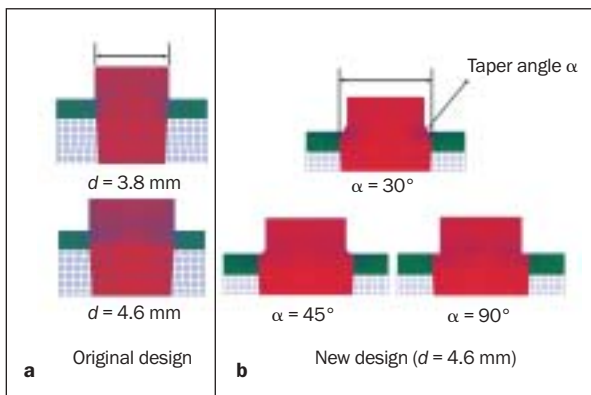

Fig 8 FE models for *(a)* the original implant design with a wider diameter and *(b)* new implant designs with tapered necks. d = diameter.

area around the neck of the implant. It can be clearly seen that, compared to the original design (Fig 1), this area has been thickened in response to the stress concentration found in the preliminary analysis.

The original implant design was then modified according to the shapes derived from the SKO process. Since 2-root designs are difficult to manufacture, and the main objective of this optimization exercise was to minimize the stresses around the neck of the implant, only the shape of the implant neck was modified. Specifically, a tapered section was introduced around the neck, as indicated by the optimization results, with different taper angles (α) being considered. As mentioned earlier, further finite FE analyses were performed for these new designs to evaluate their effectiveness in reducing the bone stresses at the implant neck. The corresponding

geometries and FE models are shown in Fig 8. For consistency, all the FE models for the different designs had a similar mesh density around the stress concentration point at the neck of the implant, with an element edge length of ~ .06 mm. These models for the modified implants were subjected to the same vertical pressure load on the occlusal surface used in the preliminary analysis. The results obtained were compared with those for the original implant (Fig 1).

All the new designs in Fig 8b have a larger neck diameter (4.6 mm) than the original design (3.8 mm) as a result of the addition of a step or taper. To compare the effectiveness of adding a taper with that of simply enlarging the diameter, a further FE model of the original implant design with a larger diameter (4.6 mm, Fig 8a) was also analyzed.

2D Evaluation of the Optimized Implant

The results for the different implant designs under axial loading are shown in Fig 9. Starting from the point of stress concentration on the top surface, the curves in these figures show the stress distributions along the interface between the implant and the crest of the cortical bone. As can be seen in the figure, the degree of stress singularity/concentration was reduced when the implants had either a larger diameter or a taper at the neck. Adding a taper was far more effective than simply increasing the diameter. Increasing the diameter of the implant reduced the peak stress by 17.2%, from 10.9 MPa to 9.0 MPa. On the other hand, for the implant with a 30-degree taper, the stress was reduced by 62.2%, from 10.9 MPa to 4.1 MPa. When the taper angle was 45 degrees, the predicted peak stress was 2.5 MPa (ie, a reduction of 77.2%). When the taper angle was 90 degrees (ie, the ideal situation, where the implant

Fig 9 Stress distributions along the bone-implant interface for different implant designs under an axial load.
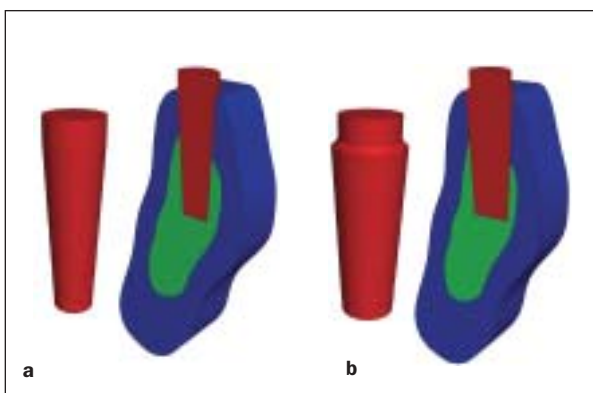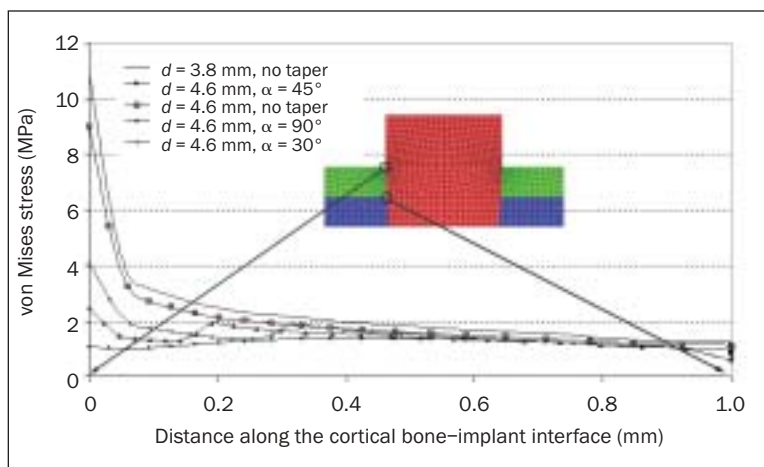

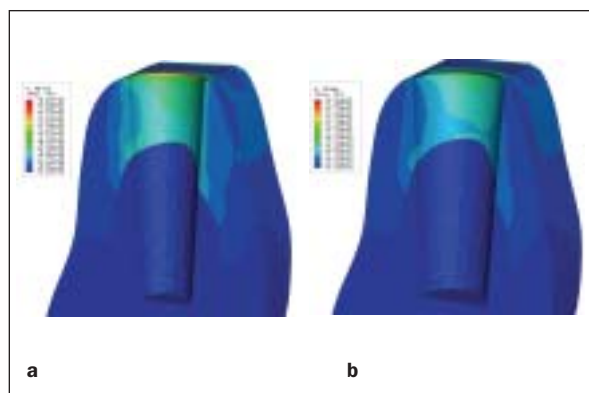Fig 10 3D FE models of (a) nonoptimized and (b) optimized implants.

Fig 11 Stress contours in the bone with (a) nonoptimized and (b) optimized implants.

shoulder is exactly level with the bone surface) the stresses along the interface were rather uniform, with values less than 2 MPa. The maximum stress was only 1.1 MPa, which represents a reduction of 90% compared with the original design.

3D Evaluation of the Optimized Implant

Two implants, 1 with the nonoptimized design (d = 3.8 mm, no taper) and 1 with the optimized design (d = 4.6 mm, α = 45 degrees), were considered using 3D models, as shown in Figs 4 and 10. Uniform axial pressure loads were first applied on the occlusal surface of the implant in both models. The application of an oblique load was then modeled.

Figure 11 shows the von Mises stress contours in the bone for both models under axial occlusal loading; to improve clarity, the implants are not shown. The peak stress of 27.8 MPa was found at the top surface of the cortical bone, close to the implant, in the original design (Fig 11a). This value was reduced to 11.3

MPa when the optimized implant was used (Fig 11b). Although the overall stress distributions of the 3D analysis are more complicated, those along the bone-implant interface within the mesiodistal plane, which includes the stress concentration at the neck position, are quite similar to those in the 2D model. However, the 3D results are higher in magnitude (Fig 12).

Figure 13 shows the stress contours in the bone for both models under oblique loading conditions. The maximum stresses were 54.0 MPa and 22.4 MPa for the original and optimized implant designs, respectively (ie, a reduction in the peak stress of ~ 49% with the optimized design).

To illustrate further the effectiveness of the optimized implant in reducing the bone stresses, Fig 14 compares the von Mises stresses in the cortical bone around the implant-neck region with the maximum diameter for both the original and optimized designs. Much lower stresses were associated with the optimized design under both axial and oblique loading.
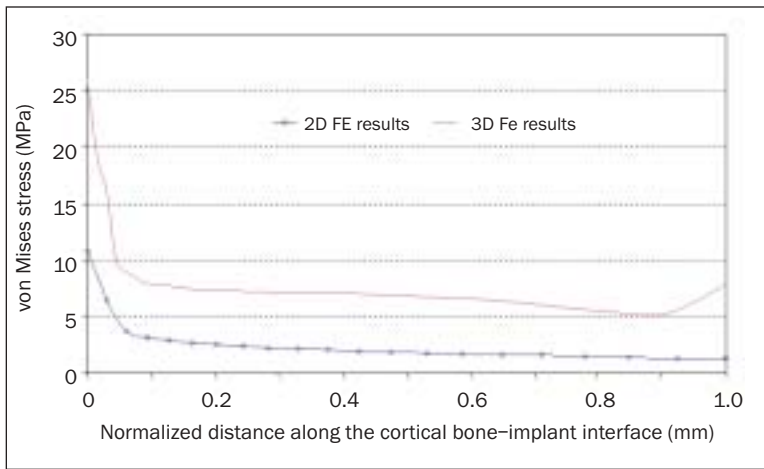
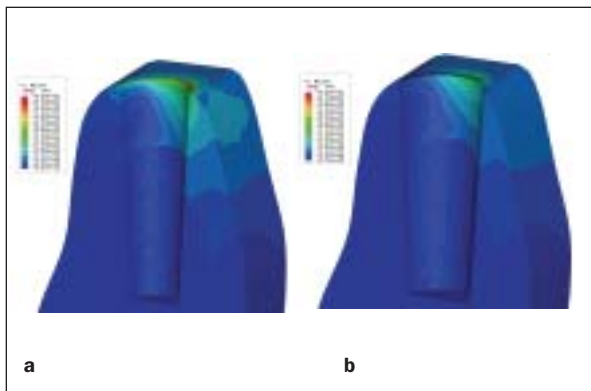Fig 12   Comparison of the stresses along the cortical bone–implant interface in the 2D and 3D FE models.

Fig 13   Stress contours in the bone with *(a)* nonoptimized and *(b)* optimized implants under oblique loading.
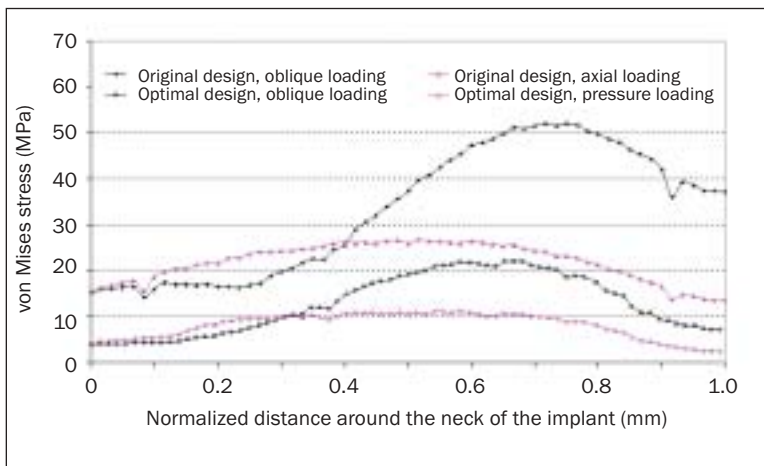

Fig 14   Comparison of the von Mises stresses around the implant neck of the cortical bone for the original and optimized designs.

DISCUSSION

The FE analysis confirmed that a stress concentration exists in the cortical bone for a generic dental implant design under occlusal loading. Similar stress concentrations around the neck area have been found in many types of implants, including cylindric, conical, stepped, tapered, screw-shaped, solid, and hollow implant designs.[16–20,32] These stress concentrations are considered a contributing factor in the loss of bone around the neck of an implant and hence can affect the success of dental restorations

supported by implants. Reducing such peak stresses is therefore an important issue in promoting and maintaining osseointegration.

A shape optimization method based on biological adaptive growth, the soft kill option proposed by Mattheck,[29] was applied to the design of dental implants to minimize the maximum bone stress due to implant loading. The improved designs obtained from the optimization process feature a wider shoulder with a taper. Subsequent FE analysis indicated that the larger implant diameter and tapered shoulder would significantly reduce the stress concentration in the cortical bone compared with conventional implants. Optimization methods can therefore be a useful tool to provide sound scientific guidelines for the design of dental implant. The optimized shapes can potentially help maintain osseointegration and prolong the survival of dental implants.

Implant diameter and length are considered the most important implant-related factors that would affect the stress concentration in the cortical bone around the neck of the implant.[17,20,21] The implant shapes derived from the optimization process seems to confirm this assertion: All the optimized designs had a wider neck diameter (4.6 mm) than the original design (3.8 mm) as a result of the addition of a step or taper. Furthermore, the evaluation analysis shows that tapering the shoulder is much more efficient than simply increasing the diameter in reducing the bone stress around the implant neck. The results also indicate that the taper angle is an important design variable in reducing the peak stress. However, extreme values for the taper angle should be avoided, as they introduce stress concentrations to the implant itself, which may cause problems relating to stability and fracture of the implant.

Although the shape optimization was carried out based on 2D models, subsequent evaluation of the new designs using 3D models confirmed the validity of the approach. More remarkably, the new designs have also been found to be effective in reducing bone stresses due to oblique loading, even though the optimization was carried out using an axial load. 2D analysis was therefore adequate for deriving the initial draft of the optimized shapes. Because of its relative simplicity, 2D also allows sensitivity studies to be carried out more easily (eg, evaluations of the effect of loading and bone quality on the optimal shape of the implant). More detailed evaluations can then be performed using more realistic 3D models based on the 2D results. However, it should be pointed out that the stresses found in the 3D models were generally higher than those found in their 2D counterparts. Thus, lower reference stresses may need to be used in the 2D optimization in order to achieve the desired stress reduction in 3D.

CONCLUSION

Alternative designs for a dental implant have been derived using shape optimization techniques based on biological adaptive growth. The new designs, which include a tapered shoulder, can significantly reduce the stress concentration at the neck of the implant.

REFERENCES

1. Weber H, Crohin CC, Fiorellini JP. A 5-year prospective clinical and radiographic study of non-submerged dental implants. Clin Oral Implants Res 2000;11:144–153.
2. Lambrecht, JT, Filippi, A, Kunzel AR, Schiel HJ. Long-term evaluation of submerged and nonsubmerged ITI solid-screw titanium implants: A 10-year life table analysis of 468 implants. Int J Oral Maxillofac Implants 2003;18:826–834.
3. Astrand P, Engquist B, Dahlgren S, Kerstin E, Feldmann H. Astra Tech and Brånemark system implants: A 5-year prospective study of marginal bone reactions. Clin Oral Implants Res 2004; 15:413–420.
4. Garcia DA, Sullivan TM, O'Neill DM. The biocompatibility of dental implant materials measured in an animal model. J Dent Res 1981;60:44–49.
5. Pham AN, Fiorellini JP, Paquette D, Williams RC, Weber HP. Longitudinal radiographic study of crestal bone levels adjacent to non-submerged dental implants. J Oral Implantol 1994;20: 26–34.
6. Callan DP, O'Mahony A, Cobb CM. Loss of crestal bone around dental implants: A retrospective study. Implant Dent 1998;7: 258–266.
7. Hermann JS, Buser D, Schenk RK, Cochran DL. Crestal bone changes around titanium implants. A histometric evaluation of unloaded non-submerged and submerged implants in the canine mandible. J Periodontol 2000;71:1412–1424.
8. Quirynen M, Naert I, van Steenberghe D. Fixture design and overload influence marginal bone loss and fixture success in the Brånemark system. Clin Oral Implants Res 1992;3:104–111.
9. Barboza EP, Caula AL, Carvalho WR. Crestal bone loss around submerged and exposed unloaded dental implants: A radiographic and microbiological descriptive study. Implant Dent 2002;11:162–169.
10. Duyck J, Naert IE, Van Oosterwyck H, et al. Biomechanics of oral implants: A review of the literature. Technol Health Care 1997;5:253–273.
11. Duyck J, Ronold HJ, Van Oosterwyck H, Naert I, Vander Sloten J, Ellingsen JE. The influence of static and dynamic loading on marginal bone reactions around osseointegrated implants: An animal experimental study. Clin Oral Implants Res 2001;12: 207–218.
12. Isidor F. Loss of osseointegration caused by occlusal load of oral implants. A clinical and radiographic study in monkeys. Clin Oral Implants Res 1996;7:143–152.
13. Isidor F. Histological evaluation of peri-implant bone at implants subjected to occlusal overload or plaque accumulation. Clin Oral Implants Res 1997;8:1–9.
14. Carr AB, Beals DW, Larsen PE. Reverse-torque failure of screw-shaped implants in baboons after 6 months of healing. Int J Oral Maxillofac Implants 1997;12:598–603.
15. Geng J, Tan KBC, Liu G. Application of finite element analysis in implant dentistry: A review of the literature. J Prosthet Dent 2001;85:585–598.

16. Kitamura E, Stegaroiu R, Nomura S, Miyakawa O. Influence of marginal bone resorption on stress around an implant—A three-dimensional finite element analysis. J Oral Rehabil 2005;32:279–286.

17. Petrie CS, Williams JL. Comparative evaluation of implant designs: Influence of diameter, length, and taper on strains in the alveolar crest: A three-dimensional finite-element analysis. Clin Oral Implants Res 2005;16:486–494.

18. Rieger MR, Mayberry M, Brose MO. Finite element analysis of six endosseous implants. J Prosthet Dent 1990;63:671–676.

19. Akagawa Y, Sato Y, Teixeira ER, Shindoi N, Wadamoto M. A mimic osseointegrated implant model for three-dimensional finite element analysis. J Oral Rehabil 2003;30:41–45.

20. Tada S, Stegaroiu R, Kitamura E, Miyakawa O, Kusakari H. Influence of implant design and bone quality on stress/strain distribution in bone around implants: A 3-dimensional finite element analysis. Int J Oral Maxillofac Implants 2003;18:357–368.

21. Petrie CS, Williams JL. Shape optimization of dental implant designs under oblique loading using the p-version finite element method. J Mechanics Med Biol 2002;2:339–345.

22. Hedia HS, Mahmoud NA. Design optimization of functionally graded dental implant. Biomed Mate Eng 2004;14:133–143.

23. Proos K, Steven G, Swain M, Ironside J. Preliminary studies on the optimum shape of dental bridges. Computer Methods in Biomechanics and Biomedical Engineering 2000;4:77–92.

24. Couegnat G, Fok SL, Cooper JE, Qualtrough AJE. Structural optimization of dental restorations using the principle of adaptive growth, accepted for publication. Dent Mater 2006; 22:3–12.

25. Mericske-Stern R, Assal P, Mericske E, Burgin W. Occlusal force and oral tactile sensibility measured in partially edentulous patients with ITI implants. Int J Oral Maxillofac Implants 1995;10:345–353.

26. Borchers L, Reichart P. Three-dimensional stress distribution around a dental implant at different stages of interface development. J Dent Res 1983;62:155–159.

27. ABAQUS version 6.5 User Manual. Pawtucket, RI: Hibbett, Karlsson and Sorensen, 2004.

28. Hassani B, Hinton E. A review of homogenization and topology optimization I-homogenization theory for media with periodic structure. Computers Structures 1998;69:707–717.

29. Mattheck C. Design in nature: Learning from trees. Springer, 1998.

30. MSC Software Corporation. MSC.Patran (r1) 2001 User's Manual. Los Angeles: MSC Software, 2001.

31. Graf H, Grassl H, Aberhard H-J. A method for measurement of occlusal forces in three directions. Helv Odont Acta 1974;18: 7–11.

32. Siegele D, Soltesz U. Numerical investigations of the influence of implant shape on stress distribution in the jaw bone. Int J Oral Maxillofac Implants 1989;4:333–340.